

16 December 2016

Selective Recovery of Metals from Geothermal Brines

Final Report

Covering the period 10/1/2014 to 9/30/2016

SRI Project P22879

Contract No. DE-EE0006747

Principal Investigator: Susanna Ventura, Senior Staff Scientist
Chemistry and Materials Laboratory
Advanced Technology and Systems Division

Contributors: Srinivas Bhamidi, Marc Hornbostel, Anoop Nagar, Elisabeth
Perea, SRI International

Submitting Organization: SRI International
333 Ravenswood Ave.
Menlo Park, CA 94025

Project Partners: Esmeralda Minerals LLC
100 West Liberty Street
10th Floor
Reno, NV 89501-1989

Nitto Innovations, Inc.
2880 Lakeside Drive, Suite 205
Santa Clara CA 95054

Prepared for: U. S. Department of Energy
DOE Geothermal Technologies Program
Golden Office/M/S:RSF/C246-5
10513 Denver West Parkway
Golden, CO 80401

DOE Project Manager Holly P. Thomas

ACKNOWLEDGMENT

This material is based upon work supported by the Department of Energy under Award Number DE-EE0006747.

DISCLAIMER

This report was prepared as an account of work sponsored by an agency of the United States Government. Neither the United States Government nor any agency thereof, nor any of their employees, makes any warranty, express or implied, or assumes any legal liability or responsibility for the accuracy, completeness, or usefulness of any information, apparatus, product, or process disclosed, or represents that its use would not infringe privately owned rights. Reference herein to any specific commercial product, process, or service by trade name, trademark, manufacturer, or otherwise does not necessarily constitute or imply endorsement, recommendation, or favoring by the United States Government or any agency thereof. The views and opinions of authors expressed herein do not necessarily state or reflect those of the United States Government or any agency thereof.

CONTENTS

| | |
|---|------------|
| Acknowledgment..... | i |
| Disclaimer | i |
| List of Figures..... | iii |
| List of Tables | iv |
| Abstract..... | v |
| Introduction..... | 1 |
| Background..... | 1 |
| Current State of the Art | 2 |
| Project Summary | 3 |
| Lithium-imprinted Polymers | 3 |
| Manganese-imprinted Polymers | 4 |
| Program Structure and Goals..... | 4 |
| Results and Discussion..... | 5 |
| Lithium-Imprinted Polymers | 5 |
| Preparation and Characterization of Li-imprinted Polymers | 5 |
| Batch Test Evaluation of Li-imprinted Polymers | 6 |
| Flow-through Tests of Li-imprinted Polymers | 7 |
| Lithium Uptake at Variable Temperature | 9 |
| Polymer Sorbent Metal Binding Selectivity | 10 |
| Lithium Separation Efficiency | 12 |
| Manganese-Imprinted Polymers..... | 13 |
| Preparation of Manganese-imprinted Polymers..... | 13 |
| Manganese-imprinted Polymers Grafted on Silica..... | 15 |
| Manganese Uptake Tests | 15 |
| Manganese Uptake at Variable Temperature..... | 16 |
| Manganese Separation Efficiency..... | 17 |
| Preliminary Cost Assessment for Separation of Lithium from Brines with Production of Lithium Carbonate | 18 |
| Conclusions and Recommendations..... | 21 |
| References..... | 22 |
| Appendix..... | 23 |

LIST OF FIGURES

| | |
|--|----|
| Figure 1. Schematic diagram of metal ions polymer imprinting. These polymers have high selectivity because of the affinity of the ligand for the imprinted metal ion and the unique size and shape of the generated cavities..... | 1 |
| Figure 2. The conventional process of lithium carbonate production based on lithium recovery from Nevada's Clayton Valley brines by solar evaporation..... | 2 |
| Figure 3. Optical microscope photograph of Li-imprinted polymer beads..... | 5 |
| Figure 4. Thermogravimetric analysis of a Li-imprinted polymer in air at a heating rate of 10°C/min. | 6 |
| Figure 5. Column setup for the flow-through evaluation of polymer sorbents..... | 8 |
| Figure 6. Lithium breakthrough profile as a function of time. | 9 |
| Figure 7. Consecutive lithium-uptake measurements of the Li-imprinted polymer 3 at 45°C and 75°C..... | 10 |
| Figure 8. Optical microscope photograph of Mn-imprinted polymer beads..... | 14 |
| Figure 9. Thermogravimetric analysis of manganese-imprinted polymer in air at the heating rate of 10°C/min..... | 14 |
| Figure 10. (a) Chemical reaction of hydroxyl terminated silica with vinyl trimethoxysilane, and (b) resulting vinyl functionalized silica beads. | 15 |
| Figure 11. Manganese uptake of imprinted polymer grafted on silica and imprinted polymer from a brine with 1500 ppm Mn ²⁺ and 2800 ppm Na ⁺ in 4.65 pH buffer at 45°C. | 16 |
| Figure 12. Batch tests of manganese uptake as a function of brine composition and temperature. | 16 |
| Figure 13. Consecutive manganese uptake measurements of polymer MEP/EGDMA 2:5 from a 1500 ppm Mn ²⁺ aqueous solution in 0.1 M NaAc buffer (pH 4.65) at 75°C in a flow-through column at 0.5 mL/min..... | 17 |
| Figure 14. Lithium extraction process. | 18 |

LIST OF TABLES

| | |
|--|----|
| Table 1. Lithium uptake of Li-imprinted polymer* from a 400-ppm Li ⁺ synthetic brine at pH 9 as a function at temperature..... | 7 |
| Table 2. Polymer Li ⁺ adsorption capacity in flow-through column..... | 9 |
| Table 3. Li ⁺ Uptake of two Li-imprinted polymers from a synthetic brine containing 412 ppm Li ⁺ , 405 ppm Na ⁺ , and 435 ppm K ⁺ at pH 9 and T=45°C..... | 10 |
| Table 4. Selectivity factors of Li-imprinted polymers at 45°C in synthetic brines at high concentrations of Na ⁺ and K ⁺ | 11 |
| Table 5. Li ⁺ Uptake of two Li-imprinted polymers from a synthetic brine containing 400 ppm Li ⁺ , 265 ppm Ca ²⁺ , and 400 ppm Mg ²⁺ at pH 9 and T=45°C..... | 12 |
| Table 6. Selectivity factors of Li-imprinted polymer determined in a brine containing Li ⁺ , Mg ²⁺ , and Ca ²⁺ at 45°C at pH 9..... | 12 |
| Table 7. Composition of synthetic brine received from INEL..... | 17 |

ABSTRACT

The objective of this project was to determine the feasibility of developing a new generation of highly selective low-cost ion-exchange resins based on metal-ion imprinted polymers for the separation of metals from geothermal fluids.

Expansion of geothermal energy production over the entire U.S. will involve exploitation of low-to-medium temperature thermal waters. Creating value streams from the recovery of critical and near-critical metals from these thermal waters will encourage geothermal expansion.

Selective extraction of metals from geothermal fluids is needed to design a cost-effective process for the recovery of lithium and manganese—two near-critical metals with well-known application in the growing lithium battery industry.

We have prepared new lithium- and manganese-imprinted polymers in the form of beads by crosslinking polymerization of a metal polymerizable chelate, where the metal acts as a template. Upon leaching out the metal template, the crosslinked polymer is expected to leave cavities defined by the ligand functional group with enhanced selectivity for binding the template metal.

We have demonstrated that lithium- and manganese-imprinted polymer beads can be used as selective solid sorbents for the extraction of lithium and manganese from brines. The polymers were tested both in batch extractions and packed bed lab-scale columns at temperatures of 45-100°C. Lithium-imprinted polymers were found to have Li^+ adsorption capacity as high as 2.8 mg Li^+/g polymer at 45°C. Manganese-imprinted polymers were found to have a Mn^{2+} adsorption capacity of more than 23 mg Mn^{2+}/g polymer at 75°C.

The Li^+ extraction efficiency of the Li-imprinted polymer was found to be more than 95% when a brine containing 390 ppm Li^+ , 410 ppm Na^+ , and 390 ppm K^+ was passed through a packed bed of the polymer in a lab-scale column at 45°C. In brines containing 360 ppm Li^+ , 10,000 ppm Na^+ , and 3,000 ppm K^+ , the Li separation efficiency of the imprinted sorbent was found to be about 30% at 45°C.

The Mn extraction efficiency of the Mn-imprinted polymer from a synthetic brine containing competing cations such as Li^+ , Na^+ , K^+ , Ca^{2+} , Mg^{2+} , and Ba^{2+} was found to be 72% at 75°C in a lab-scale column.

A preliminary process cost assessment for the recovery of lithium and production of lithium carbonate from geothermal brines was performed. We concluded that the total cost of a plant designed to process 6000 gal of brine/min is \$20,456,265 with a total annual operating costs of \$11,057,048 based on 300 days/year uptime. Assuming a conservative sale price of \$2000/ton for Li_2CO_3 , the annual revenue from the sale of Li_2CO_3 produced by this plant would exceed \$40,000,000 at a production rate of 49Kg/min for geothermal fluids containing 400 ppm Li^+ .

INTRODUCTION

BACKGROUND

Expansion of geothermal energy production over the entire U.S. will involve exploitation of low-to-medium temperature thermal waters. Creating value streams from the recovery of critical and near-critical metals from these thermal waters will encourage geothermal expansion. Subsurface fluids with both geothermal potential and lithium exist in deep geologic basins such as those in Texas, Louisiana, the Gulf Coast, Utah, and Michigan. Some of these brines also contain manganese. However, technologies must be developed to economically extract these metals from low-to-medium temperature thermal fluids.

Metal separation processes based on conventional ion-exchange resins are not desirable because of their poor specificity for metal ion binding. Alkaline and alkaline earth ions such as Na^+ , K^+ , Ca^{2+} , and Mg^{2+} are usually present in very high concentrations in geothermal fluids [1], and they effectively compete with binding of the metals of interest, reducing the resin-binding capacity and adding complexity to the separation process. Inorganic materials such as lithium manganese oxides have shown to have high Li uptake capacity; however, they have slow kinetics of absorption and desorption, requiring prolonged contact times (i.e., several hours as large particles) [2]. Furthermore, they are mostly available as powders that are expected to lead to large pressure drops in column operations and high-energy consumption.

Ion-imprinted polymers represent a new family of ion-exchange resins that promise to deliver high selectivity and binding capacity in the separation of individual metals from complex solutions, such as brines.

Ion-imprinted polymers properties have remarkably high selectivity toward the target metal ion due to the memory effect resulting from their preparation process [3]. Metal ion selectivity is imparted by: (1) the affinity of the ligand for the imprinted metal ion, and (2) the size and shape of the generated cavities. As recognition sites are generated from the self-assembly of some ligand(s) around the template metal ion (M) and subsequent crosslinking, this arrangement enables the binding sites to match the charge, size, and coordination number of the metal ion. Furthermore, the binding site geometry is preserved through the crosslinking and leaching steps, thus generating a favorable environment for the template ion rebinding (Figure 1).

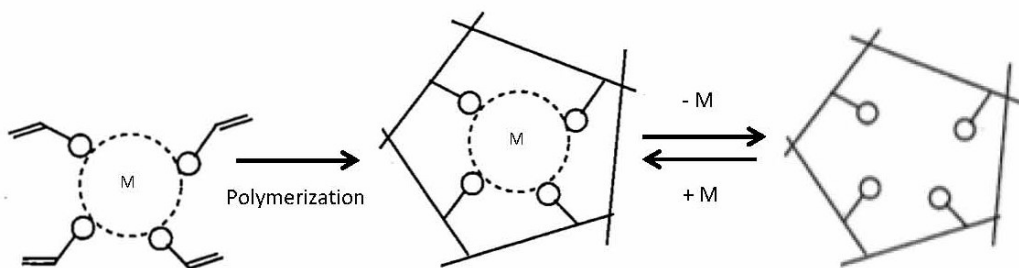


Figure 1. Schematic diagram of metal ions polymer imprinting. These polymers have high selectivity because of the affinity of the ligand for the imprinted metal ion and the unique size and shape of the generated cavities.

For this project, we have tested the feasibility of using ion-exchange resins based on ion-imprinted polymers for the separation lithium and manganese, two near-critical metals with well-known application in the growing lithium battery industry.

CURRENT STATE OF THE ART

Extraction of Li^+ from brines is currently the dominant method of Li production as compared to extraction from mineral deposits because of its more favorable processing costs. However, current processes of Li separation from brines are based on solar evaporation in ponds; therefore, they are slow (i.e., a few months), require multiple purification steps, and have low lithium recovery efficiency (< 50%) [4]. An outline of the conventional process of lithium carbonate production based on lithium recovery from Nevada's Clayton Valley brines by solar evaporation is shown in Figure 2.

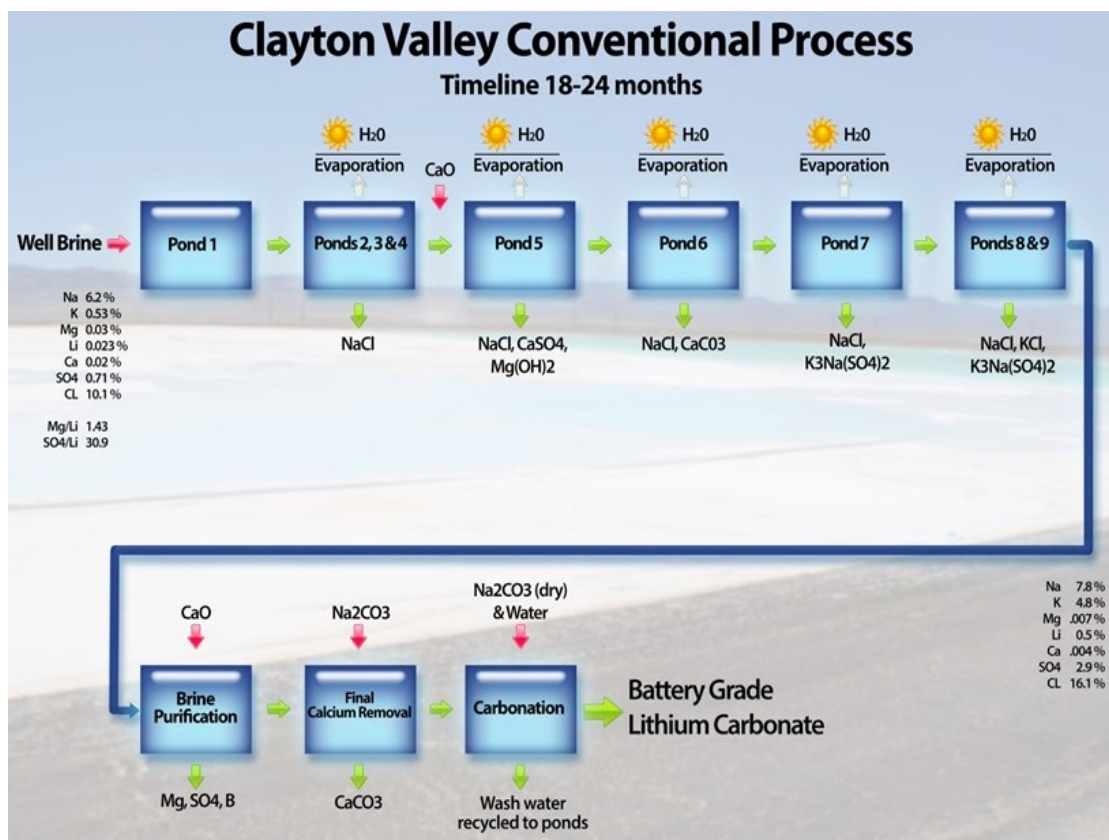


Figure 2. The conventional process of lithium carbonate production based on lithium recovery from Nevada's Clayton Valley brines by solar evaporation.

No process is currently being used for the separation of lithium or manganese from geothermal brines. Recently, Simbol Materials has demonstrated the feasibility of separating lithium from geothermal brines from the Salton Sea in a pilot plant; however, the process has not been scaled up into full-scale production yet.

PROJECT SUMMARY

The main objective of this work was to determine the feasibility of developing a new generation of highly selective, low-cost ion-exchange resins for the separation of metals from geothermal fluids. Our ion-exchange resins are based on ion-imprinted polymers chemically designed to mimic the recognition properties of biological receptors. Over the course of the project, we prepared and characterized imprinted polymers for the separation of lithium and manganese, two near-critical metals with well-known application in the growing lithium battery industry.

LITHIUM-IMPRINTED POLYMERS

Li-imprinted polymers in the form of beads were prepared by polymerization of a lithium chelate monomer, an optional co-monomer, and ethylene glycol dimethacrylate (EGDMA) as a crosslinking agent. The beads were spheres about 100 to 150 micron in diameter and were assembled in larger agglomerates with a size of 300 micron or more.

Li-imprinted polymers were shown to have Li uptake capacity up to 2.8 mg of Li/ g of polymer at 45°C. The polymer sorbents were used both in their acidic H⁺ form for lithium uptake from basic aqueous solution as well as in their Na⁺ form for lithium uptake from neutral aqueous solutions. The polymers were also tested at 75 and 100°C. The Li uptake capacity at 75°C was similar to that at 45°C, while the capacity at 100°C was somewhat lower.

The selectivity of the Li-imprinted polymers was tested in synthetic brines of different composition. In synthetic brines containing 412 ppm Li⁺, 405 ppm Na⁺, and 435 ppm K⁺, we determined that the Li-imprinted polymer binds almost exclusively Li⁺. In brines with higher concentration of Na⁺ and K⁺, the adsorption of Li⁺ by the polymer was still more favorable than that of Na⁺ and K⁺, even if the Li separation factor was lower. A Li-imprinted terpolymer prepared from a lithium chelate monomer and 2-hydroethylmethacrylate (HEMA) in the presence of a crosslinking agent was tested in flow-through columns at 45°C for Li⁺ uptake selectivity from brines containing a large excess of Na⁺ and K⁺. The Li vs. Na and Li vs. K separation factors were estimated to be 3.6 each in favor of Li adsorption when the sorbent was tested in a synthetic brine containing 360 ppm Li⁺, 10,000 ppm Na⁺, and 3000 ppm K⁺ at pH 8. Other Li-imprinted polymers were tested for their selectivity under the same conditions. We found that the Li vs. Na separation factor varied within 2.3-3.7 and the Li vs. K separation factor varied within 3.2-4.5, depending on the polymer composition. In conclusion, for all Li-imprinted polymers tested, the adsorption of Li⁺ was favored as compared to that of Na⁺ and K⁺. Furthermore, the Li⁺ adsorption selectivity of Li-imprinted polymers was found to be significantly higher than that of conventional sulfonated ion exchange resins, for which selectivity separation factors of 0.4-0.6 for Li vs. Na and 0.22-0.4 for Li vs. K have been reported [5].

The ability of the Li-imprinted polymer to adsorb lithium in the presence of similar concentrations of Ca²⁺ and Mg²⁺ was evaluated in batch tests. In brines containing 400 ppm Li⁺, 400 ppm Mg²⁺, and 265 ppm Ca²⁺, we found that the Li vs. Mg and Li vs. Ca separation factors were less than 1, indicating the Li⁺ is less favorably adsorbed than Ca²⁺ and Mg²⁺. Therefore, it is expected that Ca²⁺ and Mg²⁺ will interfere with the adsorption of Li⁺ on the polymer sorbent and will need to be separated before Li⁺ extraction is conducted.

In agreement with the separation factors determined, the Li separation efficiency of Li-imprinted polymers from brines with similar concentrations of lithium, sodium, and potassium was found to be more than 95% when tested in a flow-through packed bed. In a similar test, the Li separation efficiency from brines containing 360 ppm Li^+ , 10,000 ppm Na^+ , and 3,000 ppm K^+ was found to be about 30%.

A Li-imprinted polymer was tested for its Li uptake for three consecutive cycles at 45°C and two more cycles at 75°C. The uptake measurement for the five consecutive tests did not vary significantly and averaged 0.92 mg Li^+/g polymer at 45°C and 0.89 mg Li^+/g polymer at 75°C.

MANGANESE-IMPRINTED POLYMERS

Mn-imprinted polymers in the form of beads were prepared by polymerization of a manganese chelating monomer, a manganese compound such as MnCl_2 , and ethylene glycol dimethacrylate (EGDMA) as crosslinking agent. We have demonstrated manganese uptake capacity exceeding 22 mg of Mn^{2+}/g of polymer sorbent in batch test experiments at 45°C.

A representative Mn-imprinted copolymer was further tested four consecutive times for its Mn^{2+} uptake in a jacketed flow-through packed bed column at 75°C. The manganese uptake capacity did not change significantly for the four cycles with an average capacity of 23.1 mg Mn^{2+}/g polymer.

The Mn^{2+} separation efficiency of this polymer tested at 75°C from an INEL synthetic brine containing competing cations such as Li^+ , Na^+ , K^+ , Ca^{2+} , Mg^{2+} , and Ba^{2+} was found to be 72%.

A preliminary process cost assessment for the recovery of lithium and production of lithium carbonate from geothermal brines was performed. We concluded that the total cost of a plant designed to process 6000 gal of brine/min is \$20,456,265 with a total annual operating costs of \$11,057,048 based on 300 days/year uptime. Assuming a conservative sale price of \$2000/ton for Li_2CO_3 , the annual revenue from the sale of Li_2CO_3 produced by this plant would exceed \$40,000,000 at a production rate of 49Kg/min.

PROGRAM STRUCTURE AND GOALS

The main tasks of our 2-year project development include: (1) synthesis and characterization of the lithium and manganese imprinted polymers, (2) batch test of the imprinted polymers to determine their metal uptake capacity, and (3) flow-through tests of the packed bed of the metal imprinted polymers. Tests were performed in the temperature range of 45-100°C using synthetic brines.

Our goal was to develop ion-imprinted polymers for lithium and manganese recovery that are more efficient, selective, and durable than existing materials. Our target performance goals were:

- Lithium-imprinted polymers with lithium separation efficiency higher than 95% and capacity greater than 4 mg Li^+/g sorbent up at 45-100°C.
- Manganese-imprinted polymers with manganese separation efficiency higher than 90% and capacity greater than 27 mg Mn^{2+}/g sorbent at 45-100°C.

RESULTS AND DISCUSSION

LITHIUM-IMPRINTED POLYMERS

Preparation and Characterization of Li-imprinted Polymers

Li-imprinted polymers were prepared in the form of beads by suspension polymerization of a mixture of the following:

- Lithium chelate monomer
- Co-monomer
- Ethylene glycol dimethacrylate as crosslinking agent
- Porogen solvent
- Radical initiator azobisisobutyronitrile (AIBN).

Several Li-imprinted polymers were prepared by varying the amount of crosslinking agent and therefore the degree of crosslinking, and by changing the nature of the comonomer.

An optical microscope photograph of typical Li-imprinted macrobeads is shown in Figure 2. Individual polymer beads (100-150 micron diameter) are assembled in larger agglomerates (300 micron or more).

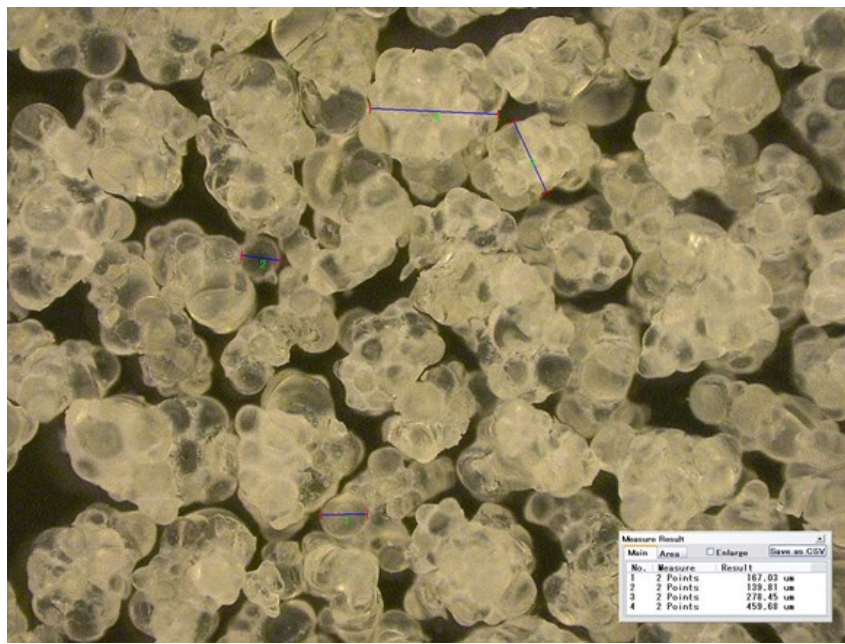


Figure 3. Optical microscope photograph of Li-imprinted polymer beads.

After polymerization was complete, the polymer beads were isolated by filtration and transferred into a Soxhlet extractor, where they were extensively washed with a mixture of acetone and chloroform to extract any unreacted monomer for over 15 hours. After drying, the Li-containing

polymer was under vacuum at 70°C for over 15 hours, transferred to a flask, and stirred with 0.1 M HCl to remove the bound lithium and convert the polymer into its H⁺-form.

Polymerization conditions, such as the co-solvent system, stirring rate, and temperature, were varied to ensure that the polymers were prepared in the form of macrobeads for use in packed-bed column separation. The macrobeads were tested by Brunauer-Emmett-Teller (BET) analysis and found to have high surface area of about 100-250 m²/g.

The crosslinked polymers were found to be thermally stable as characterized by TGA by heating in air at a rate of 10°C/min. In Figure 3, the polymer weight loss of a Li-imprinted polymer is plotted as a function of the temperature, showing an inset of decomposition is at 243.9°C.

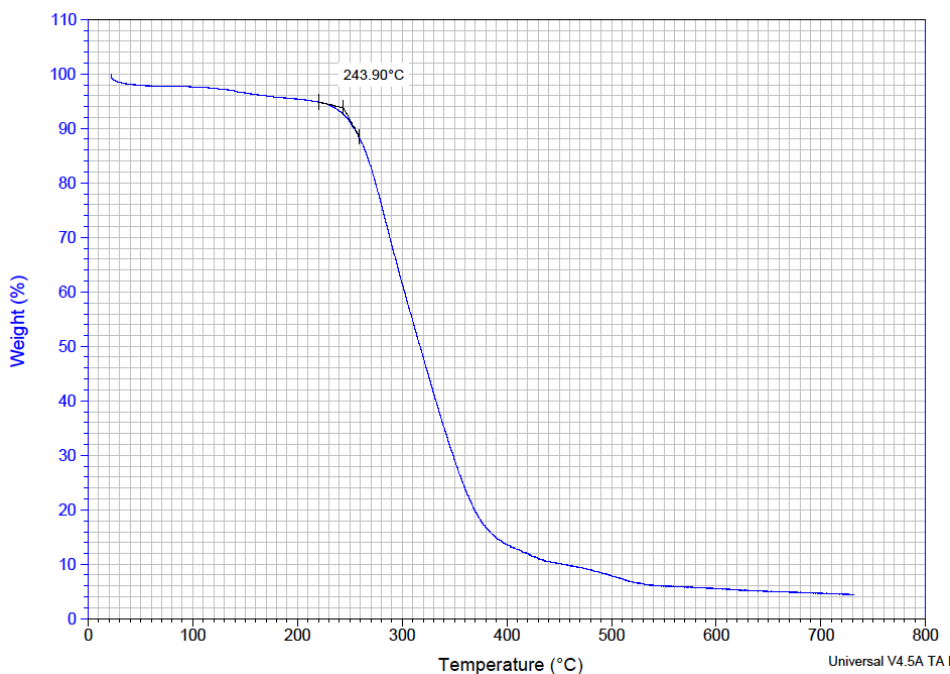


Figure 4. Thermogravimetric analysis of a Li-imprinted polymer in air at a heating rate of 10°C/min.

Batch Test Evaluation of Li-imprinted Polymers

The polymer's metal binding capacity was evaluated by performing batch adsorption tests at variable temperature. We chose to perform initial tests at 45°C since this is the exit temperature of the geothermal fluid of current operating geothermal binary systems. Metal uptake at 75°C and 100°C was also evaluated.

A portion of the dried polymer (125 or 250 mg) was contacted with a buffer solution of known composition (5 or 10 mL) and gently shaken for 30-60 minutes at the desired temperature.

Polymer metal uptake was calculated by comparing the metal concentration in the initial solution (C_i) and the metal concentration in the solution after polymer treatment (C_f). The concentration of the metal ions in solution was determined by inductively coupled plasma optical emission spectrometry (ICP-OES). Metal uptake was calculated according to the following equation:

$$\text{Metal uptake (mg/g)} = \frac{V_{\text{solution}} (L) C_i (\text{mg/L}) - C_f (\text{mg/L})}{W_{\text{polymer}} (\text{g})}$$

where W is the weight of the polymer used for the test, and V is the volume of the solution contacted with the polymer.

The metal uptake capacity of the polymer varied as a function of the composition and degree of crosslinking. Tests were performed both in pH 9 buffer solutions of 0.1 M NH₄Cl/NH₄OH and in aqueous solutions with a pH of about 7.

Li uptake as high as 2.8 mg Li⁺/g polymer was found for the best-performing Li-imprinted polymers tested in an aqueous solution containing 390 ppm Li at 45°C both at pH 7 and pH 9.

One of the Li-imprinted polymers was also tested for its uptake from a pH 9 buffer solution of 0.1 M NH₄Cl/NH₄OH containing 400-ppm Li⁺ content as function of temperature. We found that the lithium uptake was 2.1-2 mg Li⁺/g polymer at 45 and 75°C, but lower at 100°C. More tests should be performed to assess whether the reduced capacity at 100°C is due to lower binding constant or polymer instability at this temperature.

Table 1. Lithium uptake of Li-imprinted polymer* from a 400-ppm Li⁺ synthetic brine at pH 9 as a function at temperature.

| Li ⁺ uptake (mg Li/g polymer) | Li ⁺ uptake (meq Li /g polymer) | Temperature (°C) | Contact time (min) |
|---|---|------------------|--------------------|
| 2.1 | 0.30 | 45 | 30 |
| 2 | 0.29 | 75 | 30 |
| 1.6 | 0.23 | 100 | 30 |

* Polymer 1 [2-(methacryloxy)ethyl phosphate (MEP) terpolymer]

Flow-through Tests of Li-imprinted Polymers

We tested selected Li-imprinted polymers in flow-through packed bed columns over a range of temperatures to evaluate their metal-binding characteristics under dynamic conditions.

The polymer to be tested was transferred in a jacketed column 10-mm wide and 30-cm long, heated at the desired temperature.

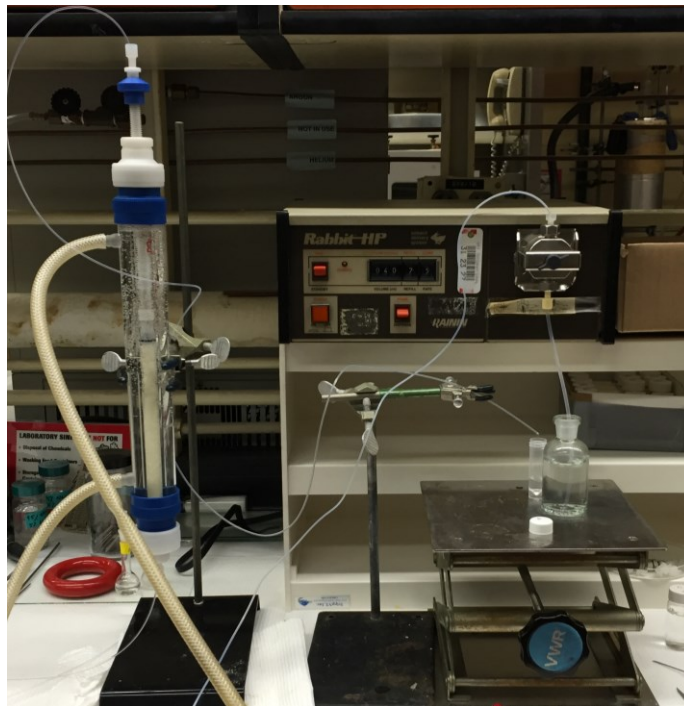


Figure 5. Column setup for the flow-through evaluation of polymer sorbents.

Li-imprinted copolymers of different composition were tested according to the following protocol at 45°C at a flow rate of 0.5 mL/min:

1. The polymers were loaded in the column in their H⁺ form.
2. An aqueous solution of 0.1 M NaOH was passed through the column to exchange H⁺ with Na⁺.
3. The polymer was washed with a large excess of water to remove any free Na⁺.
4. A Li⁺-containing brine was passed through the column to capture Li⁺. Samples of the eluent were collected at regular time intervals and tested for their Li⁺ content.

The brine tested contained 410 ppm of Li⁺ at pH 7, and several samples of the eluent were collected at regular time interval to establish the Li⁺ breakthrough profile. The Li content of these samples was determined by ion exchange chromatography and ICP-OES.

Once we determined that the sorbent was fully saturated by Li⁺, it was rinsed with water to wash out any free unbound Li⁺ in the column. Finally, a known volume of 0.5 M HCl was passed through the column to remove all the Li⁺. By testing the Li concentration in the acidic solution, we determined the Li-binding capacity of the polymer sorbent.

The Li-binding capacity of the polymer in the packed bed flow-through column was similar to the capacity obtained from batch tests.

Table 2. Polymer Li⁺ adsorption capacity in flow-through column.

| Polymer | Li uptake (mg Li /g polymer) |
|----------------------------|------------------------------|
| <u>1</u> (MEP terpolymer) | 1.85 |
| <u>3</u> (HEMA terpolymer) | 1.4 |

Note: Column separation conditions: T= 45°C, 0.5 mL/min eluent flow rate

A representative lithium breakthrough profile for a Li-imprinted polymer as function of elution time is shown below.

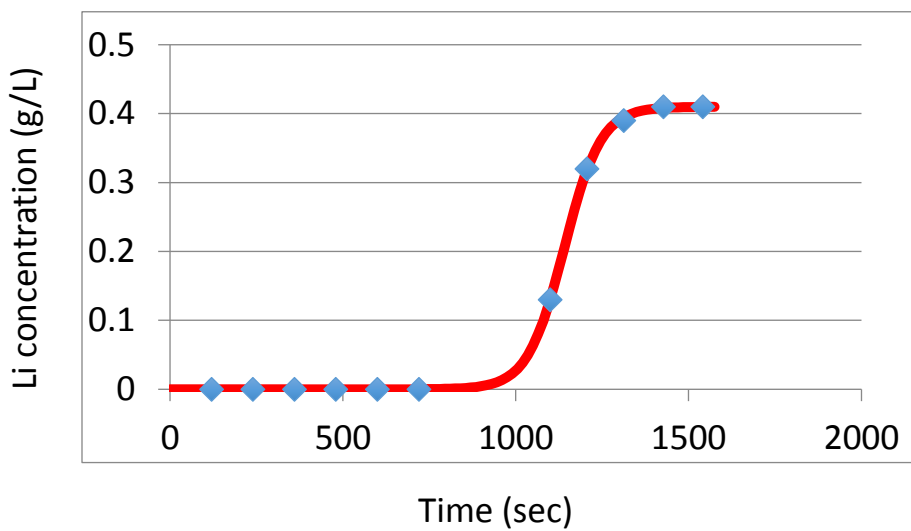


Figure 6. Lithium breakthrough profile as a function of time.

The lithium breakthrough profile is quite sharp, thus indicating that the kinetics of lithium exchange are quite fast.

Lithium Uptake at Variable Temperature

The Li-imprinted polymer 3 (HEMA terpolymer) was tested in a flow-through column for its lithium uptake at 45°C and 75°C from a brine solution composed of 410 ppm of Li⁺ in a pH buffer solution of 0.1 M NH₄Cl/NH₄OH. Three consecutive lithium uptake tests were performed at 45°C, followed by two tests at 75°C. After each lithium uptake test, the column was rinsed with water. The lithium uptake measurements for the five consecutive tests did not vary significantly and averaged 0.92 mg Li⁺/g polymer at 45°C and 0.89 mg Li⁺/g polymer at 75°C.

It should be noted the capacity of these polymers is somehow lower than previous data (~ 0.9 mg Li⁺/g polymer vs. 1.4 mg Li⁺/g polymer), likely because the metal uptake tests were performed in the presence of a large concentration of NH₄⁺, which may interfere with the binding of Li⁺.

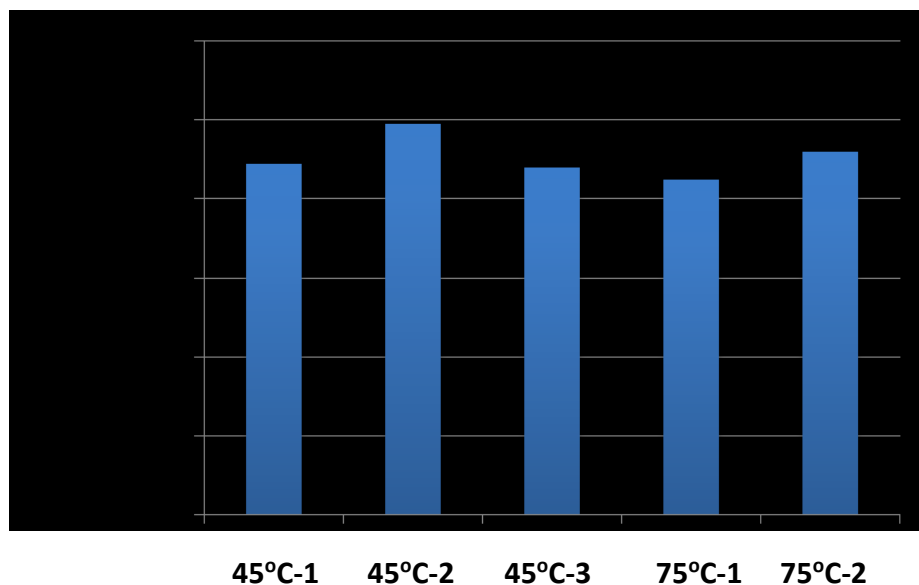


Figure 7. Consecutive lithium-uptake measurements of the Li-imprinted polymer 3 at 45°C and 75°C.

Polymer Sorbent Metal Binding Selectivity

Li-imprinted polymers were tested for their separation factors in the presence of other metals by testing the lithium and other metal uptake from synthetic brines with known composition according to batch tests as well as column flow-through tests. The selectivity factors were calculated as follows:

$$\text{Selectivity separation factor } \alpha_{\text{Li/M}} = Q_{\text{Li}}/C_{\text{Li}} * C_{\text{M}}/Q_{\text{M}}$$

where Q_{Li} and Q_{M} are the adsorption capacities of Li and M in the polymer (meq /g polymer), while C_{Li} and C_{M} are the concentrations of Li and M in the brine (meq/L brine) tested.

Li-imprinted polymers were tested for their metal uptake capacity in the presence of Li^+ , Na^+ , and K^+ at 45°C in batch experiments. A synthetic brine containing 412 ppm Li^+ , 405 ppm Na^+ , and 435 ppm K^+ was prepared from LiCl , NaCl , and KCl in a pH 9 buffer solution of 0.1 M $\text{NH}_4\text{Cl}/\text{NH}_4\text{OH}$ (corresponding to more than 5300 ppm of NH_4^+). Li-imprinted polymer were found to adsorb Li almost exclusively according to the data shown in Table 2.

Table 3. Li^+ Uptake of two Li-imprinted polymers from a synthetic brine containing 412 ppm Li^+ , 405 ppm Na^+ , and 435 ppm K^+ at pH 9 and T=45°C.

| Li-imprinted Polymer | Li^+ uptake (meq Li /g polymer) | Na^+ uptake (meq Li /g polymer) | K^+ uptake (meq Li /g polymer) |
|---------------------------|--|--|---|
| <u>1</u> (MEP terpolymer) | 0.27 | 0.01 | 0.01 |
| <u>2</u> (copolymer) | 0.21 | Not detectable | <0.01 |

Note: The brine also contained 5300 ppm of NH_4^+

In brines with higher concentrations of Na^+ and K^+ , the adsorption of Li^+ by the polymer was still more favorable than that of Na^+ and K^+ , but the Li separation factors were lower. Various Li-imprinted polymers were tested for their Li binding properties from brines containing 360 ppm Li^+ , 10,000 ppm Na^+ , and 3000 ppm K^+ .

The polymers were tested in flow-through columns according to the following protocol:

1. The polymers were loaded in the column in their H^+ form.
2. An aqueous solution of 0.1 M NaOH was passed through the column to exchange H^+ with Na^+ .
3. The polymer was washed with a large excess of water to remove any free Na^+ .
4. A large excess (100 mL) of a brine containing 360 ppm Li^+ , 10,000 ppm Na^+ , and 3000 ppm K^+ was passed through the column.
5. The sorbent was rinsed with about 150 mL of deionized water to remove any unbound metal ions.
6. 0.5 M HCl (50 mL) was eluted through the column to desorb the bound metal ions and regenerate the sorbent.

The acidic eluent was tested for its Li, Na, and K content to assess the polymer Li binding selectivity. Table 3 shows the selectivity factors for two analogous polymers with different degrees of crosslinking, with polymer 3 having a higher degree of crosslinking. It should be noted that an excess of 0.5 M HCl was used to desorb the bound metals, and the entire acid solution was collected without separating it in fractions; therefore, the resulting metal concentration in the eluent is quite low.

Table 4. Selectivity factors of Li-imprinted polymers at 45°C in synthetic brines at high concentrations of Na and K.

| Li-imprinted Polymer | Selectivity Separation Factor | |
|----------------------------|--------------------------------|-------------------------------|
| | $\alpha_{\text{Li}/\text{Na}}$ | $\alpha_{\text{Li}/\text{K}}$ |
| <u>3</u> (HEMA terpolymer) | 3.1 | 3.2 |
| <u>4</u> (HEMA terpolymer) | 3.6 | 3.6 |
| <u>2</u> (copolymer) | 3.7* | 4.5* |
| <u>1</u> (MEP terpolymer) | 2.3** | |

Note: Unless otherwise noted, the brine composition was 360 ppm Li^+ , 10,000 ppm Na^+ , 3000 ppm K^+ ; pH 8, T=45C.

(*) batch test

(**) brine composition 7968 ppm Na^+ , 420 ppm Li^+

As shown in Table 4, the Li vs. Na selectivity varied between 2.3-3.7, and the Li vs. K selectivity separation factor varied within 3.2-4.5, depending on the polymer composition, indicating that Li^+ is preferably adsorbed by the polymer as compared to Na^+ and K^+ . It should be noted that the

Li^+ adsorption selectivity of these polymers is significantly higher than that of conventional sulfonated ion exchange resins, which have poor selectivity for lithium adsorption and have been reported to have selectivity separation factors that vary from 0.4 to 0.6 for Li vs. Na and from 0.22 to 0.4 for Li vs. K .

The selectivity of a representative Li-imprinted polymer in the presence of Ca^{2+} and Mg^{2+} was tested in batch experiments. Table 5 shows the metal uptake capacity of the polymer in a brine containing 400 ppm Li^+ , 400 ppm Mg^{2+} , and 265 ppm Ca^{2+} . From these data, the Li vs. Mg and Li vs. Ca separation factors were determined to be less than 1, indicating the Li^+ is less favorably adsorbed than Ca^{2+} and Mg^{2+} . Therefore, Ca^{2+} and Mg^{2+} will interfere with the adsorption of lithium by the polymer; therefore, they will need to be separated before lithium extraction is conducted.

Table 5. Li^+ Uptake of two Li-imprinted polymers from a synthetic brine containing 400 ppm Li , 265 ppm Ca , and 400 ppm Mg at pH 9 and $T=45^\circ\text{C}$.

| Li-imprinted Polymer | Li^+ Uptake (meq Li^+ /g polymer) | Ca^{2+} Uptake (meq Ca^{2+} /g polymer) | Mg^{2+} Uptake (meq Mg^{2+} /g polymer) |
|---------------------------|---|---|---|
| <u>1</u> (MEP terpolymer) | 0.21 | 0.12 | 0.47 |

Note: The brine contained also 5300 ppm of NH_4^+ .

Table 6. Selectivity factors of Li-imprinted polymer determined in a brine containing Li^+ , Mg^{2+} , and Ca^{2+} at 45°C at pH 9.

| Li-imprinted Polymer | Selectivity Separation Factor ($\alpha_{\text{Li/Ca}}$) | Selectivity Separation Factor ($\alpha_{\text{Li/Mg}}$) |
|-------------------------|--|--|
| <u>1</u> | 0.4 | 0.25 |

Note: The brine contained also 5300 ppm of NH_4^+ .

Lithium Separation Efficiency

A representative Li-imprinted polymer was tested in a flow-through column for its lithium separation efficiency at 45°C .

A fixed volume of brine containing an amount of lithium corresponding to the polymer capacity was passed through the column. The polymer sorbent was then rinsed with water to wash out any unbound lithium ions. No lithium was detected in the water, indicating that all the lithium ions were extracted by the polymer. The polymer was then regenerated with 0.5 M HCl, and samples of the acidic eluent are currently being tested for their Li content by ICP-OES.

To assess the Li separation efficiency in more complex brines, similar extraction experiments were performed using brines with the composition shown as follows:

- Brine 1: 390 ppm Li^+ , 410 ppm Na^+ , 390 ppm K^+
- Brine 2: 360 ppm Li^+ , 10,000 ppm Na^+ , 3000 ppm K^+ .

After the brine was eluted through the column, the polymer sorbent was rinsed with water and regenerated with 0.5M HCl to determine the Li separation efficiency. Samples of the acidic eluent are currently being tested for their Li content by ICP-OES.

With brine 1, we determined that more than 95% of the Li was captured by the polymer and released upon regeneration with 0.5 M HCl.

With brine 2, we determined that 30% of the Li was captured by the polymer and released upon regeneration with 0.5 M HCl.

Both results are consistent with the Li selectivity factors previously determined for the imprinted polymer in the two brine compositions.

MANGANESE-IMPRINTED POLYMERS

Preparation of Manganese-imprinted Polymers

Manganese-imprinted polymers were prepared in the form of beads by suspension polymerization of the following:

- Functional monomer with Mn²⁺ binding properties
- Manganese chloride
- Ethylene glycol dimethacrylate as crosslinking agent
- Porogen solvent
- Radical initiator azobisisobutyronitrile (AIBN).

Several Mn-imprinted polymers were prepared by varying the relative amount of functional monomer and crosslinking agent.

An optical microscope photograph of typical Mn-imprinted macrobeads with diameter of 220 micron and more is shown in Figure 8.

After the polymerization was completed, the polymer beads were isolated by filtration and transferred into a Soxhlet extractor, where they were extensively washed with a mixture of acetone and chloroform to extract any unreacted monomer for over 15 hours. After drying the Mn-containing polymer under vacuum at 70°C for over 15 hours, it was transferred in a flask and stirred with 0.1 M HCl to remove the bound manganese and convert the polymer into its H⁺-form.

Polymerization conditions, such as co-solvent system, stirring rate, and temperature, were varied to prepare the polymers in the form of macrobeads for use in packed bed column separation. The macrobeads were tested by BET analysis and found to have high surface area in excess of 200 m²/g.

The crosslinked polymers were found to be thermally stable as characterized by TGA by heating them in air at a rate of 10°C/min. In Figure 9, the polymer weight loss of a Li-imprinted polymer is plotted as a function of the temperature, showing an onset of decomposition is at 251.99°C.



Figure 8. Optical microscope photograph of Mn-imprinted polymer beads.

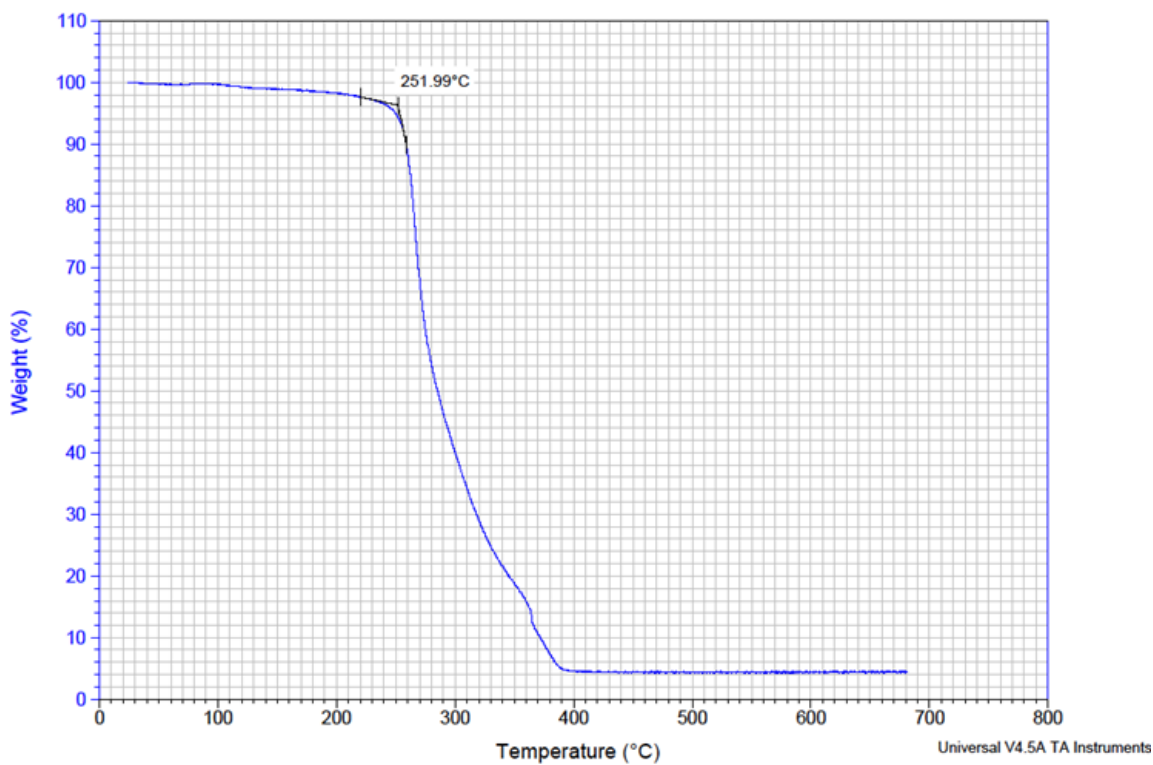


Figure 9. Thermogravimetric analysis of manganese-imprinted polymer in air at the heating rate of 10°C/min.

Manganese-imprinted Polymers Grafted on Silica

Additionally, we prepared Mn-imprinted polymers grafted on silica particles. Silica particles act as solid support of the imprinted polymer and offer excellent mechanical stability to the resulting separation media.

Before grafting the Mn-imprinted polymer on silica beads ((SiliaFlash G60, 60-200 micron), the beads were first reacted with vinyl trimethoxysilane to functionalize the free hydroxyl groups on the surface of the high-surface-area porous silica beads with formation of vinyl end groups. The reaction takes place as shown in Figure 10.

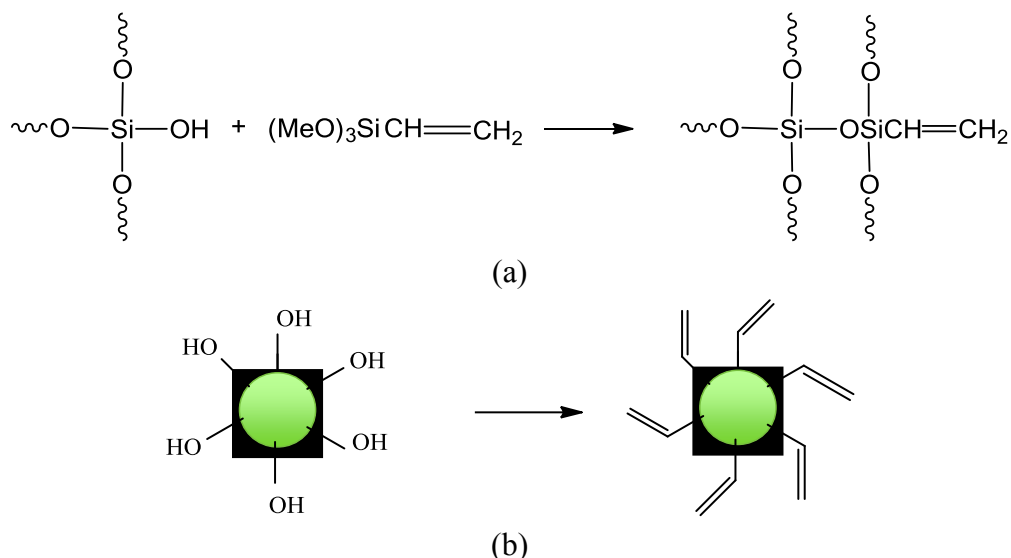


Figure 10. (a) Chemical reaction of hydroxyl terminated silica with vinyl trimethoxysilane, and (b) resulting vinyl functionalized silica beads.

The vinyl groups allow grafting of the imprinted polymer directly on the silica particles. Furthermore, the binding capacity of the imprinted polymers grafted on silica can be adjusted by varying the silica particle size and surface area as well by the weight ratio of monomers:silica. Smaller quantities of silica support are sufficient if the silica has small particle size and high surface area.

Thus, a Mn-imprinted polymer grafted on silica was prepared by reaction of a functional monomer with Mn-binding properties, Mn chloride, and ethylene glycol dimethacrylate as crosslinking agent in dimethylformamide using AIBN as the radical initiator.

The resulting silica-grafted polymer was then treated with excess 0.1 M $HCl_{(aq)}$ to remove the manganese ions bound to the polymer, and to generate the corresponding Mn-imprinted polymer.

Manganese Uptake Tests

We screened the polymers we prepared for their Mn^{2+} uptake in batch tests. The best manganese uptake was found to be 19.3 mg Mn^{2+} /g polymer from a brine containing 1500 ppm Mn^{2+} and 2800 ppm Na^+ in 4.65 pH buffer at 45°C.

The manganese uptake capacity of imprinted polymers grafted on silica was comparable to that of equivalent polymers without silica after the amount of silica within the polymer was discounted. Figure 10 illustrates the Mn^{2+} uptake for an imprinted polymer grafted on silica and imprinted polymer without any silica with the same composition tested under similar conditions.

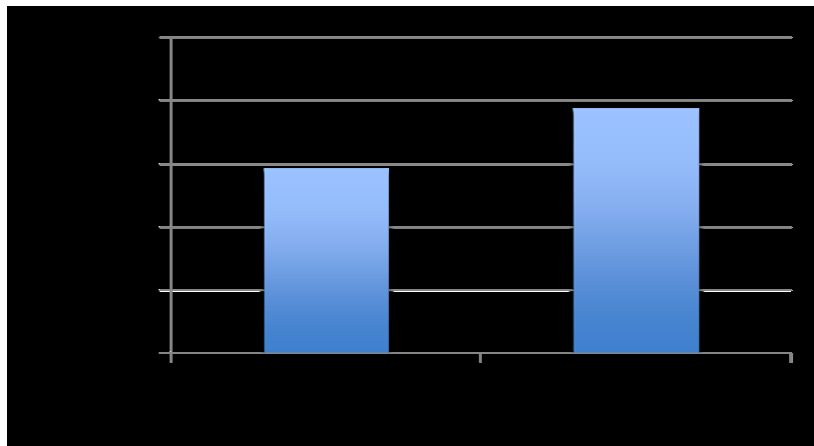


Figure 11. Manganese (II) uptake of imprinted polymer grafted on silica and imprinted polymer from a brine with 1500 ppm Mn^{2+} and 2800 ppm Na^+ in 4.65 pH buffer at 45°C.

Manganese Uptake at Variable Temperature

The imprinted polymer was tested for its manganese uptake at variable temperature. The results of batch tests conducted at 45°C, 75°C, and 100°C in aqueous solution containing 1500 ppm Mn^{2+} , 2800 ppm Na^+ , and 1500 ppm of Mn^{2+} in 3% NaCl aqueous solution are shown below.

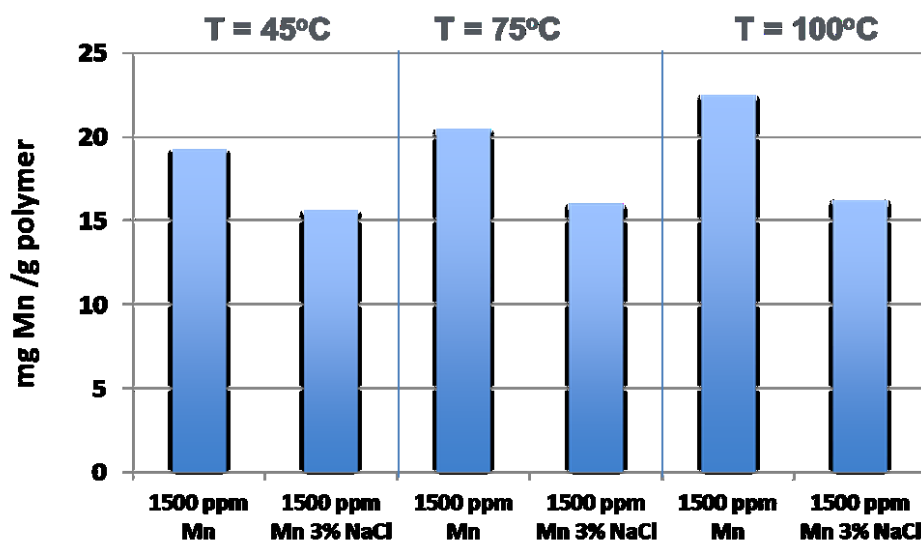


Figure 12. Batch tests of manganese(II) uptake as a function of brine composition and temperature.

The Mn-imprinted polymer was further tested four consecutive times for its Mn^{2+} uptake from a solution of 1500 ppm Mn^{2+} in a jacketed flow-through column held at 75°C. As indicated in Figure 13, the manganese uptake was quite constant and averaged 23.1 mg Mn^{2+} /g polymer.

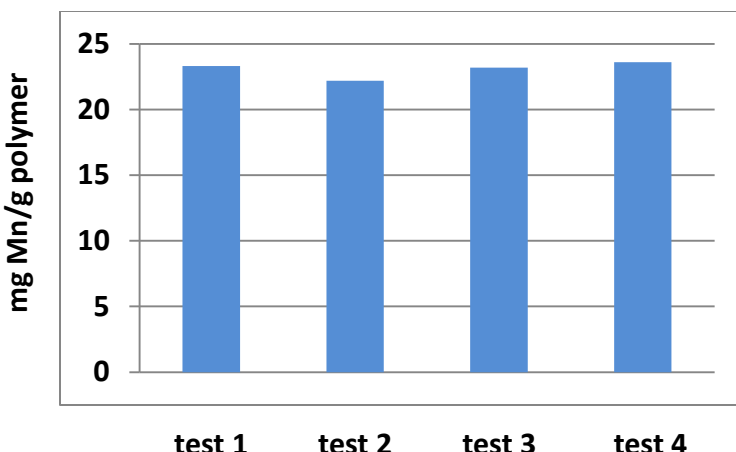


Figure 13. Consecutive manganese uptake measurements of polymer MEP/EGDMA 2:5 from a 1500 ppm Mn²⁺ aqueous solution in 0.1 M NaAc buffer (pH 4.65) at 75°C in a flow-through column at 0.5 mL/min.

Manganese Separation Efficiency

The Mn-imprinted polymer was tested in a flow-through column for its manganese separation efficiency from a brine we received from the Idaho National Engineering Laboratory (INEL); the brine's composition is summarized in Table 7.

Table 7. Composition of synthetic brine received from INEL.

| Simple Brine with Li ⁺ , Mn ²⁺ | Concentration (mg/L) |
|--|----------------------|
| Na ⁺ | 19000 |
| Ca ²⁺ | 200 |
| Mg ²⁺ | 100 |
| K ⁺ | 700 |
| Ba ²⁺ | 20 |
| Li ⁺ | 400 |
| Mn ²⁺ | 1320(*) |
| Cl ⁻ | 34440 |
| TDS | 55500 |

(*) concentration tested by ICP-OES at SRI.

Ten mL of the INEL brine were passed through a column containing 4.5 g of the polymer sorbent at a flow rate of 0.5 mL/min and T=75°C. The polymer sorbent was then rinsed with water to wash out any unbound ions. The polymer was then regenerated with 0.25 M HCl, and samples of the acidic eluent were tested for their Li content by ICP-OES, indicating that 72% of Mn²⁺ had been separated.

PRELIMINARY COST ASSESSMENT FOR SEPARATION OF LITHIUM FROM BRINES WITH PRODUCTION OF LITHIUM CARBONATE

A simplified model of the proposed process for the extraction of lithium from geothermal brines is shown in Figure 14.

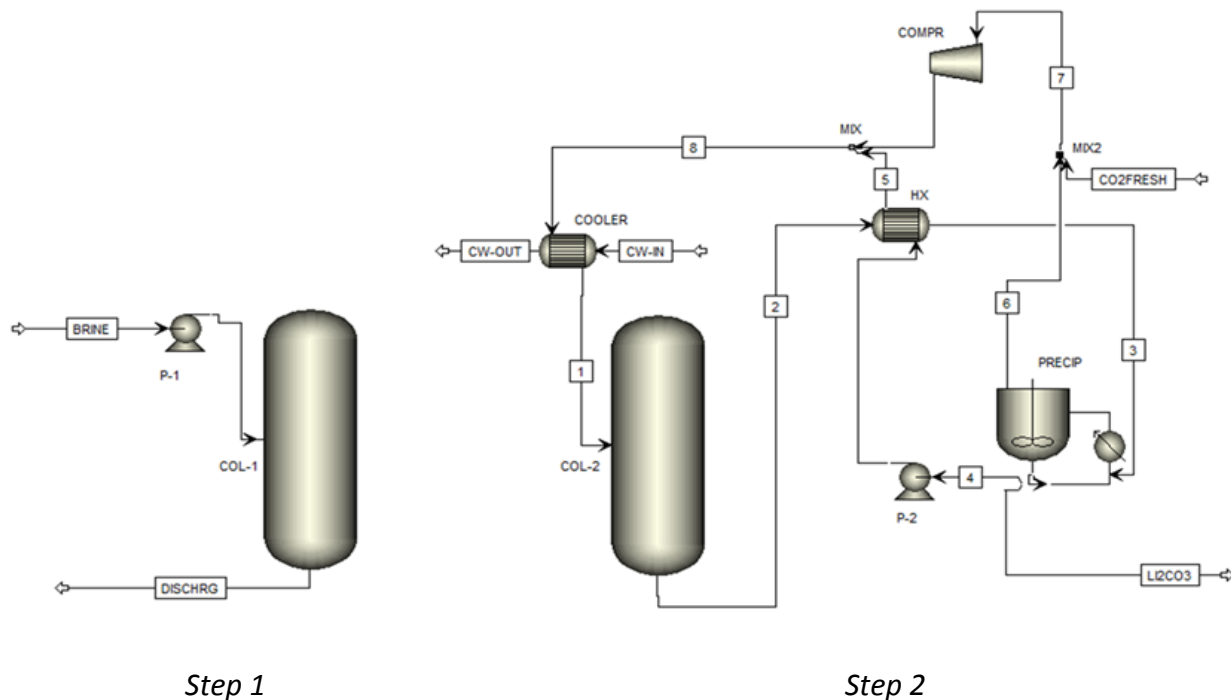


Figure 14. Lithium extraction process.

Lithium is isolated according to two main steps:

- *Step 1*: Extraction of lithium by the imprinted sorbent,
- *Step 2*: Regeneration of the sorbent by treatment of CO₂ in water with formation of Li₂CO₃.

It should be noted that the process economics are evaluated based on the sorbent regeneration the with CO₂, instead of the conventional regeneration process based on the use of aqueous HCl we have used during the course of this project. The feasibility of the CO₂ regeneration has been demonstrated in our laboratories, and it is expected to be more cost effective for the direct production of Li₂CO₃.

In our cost analysis, we also included the following two pretreatments not shown in Figure 14:

- (1) Microfiltration to separate any solids present.
- (2) Membrane nanofiltration to separate multivalent ions.

After pretreatment, lithium is extracted by passing the brine through the sorbent in column 1 (Figure 14, Step 1). The sorbent is then regenerated using moderate-pressure CO₂ gas to produce carbonic acid, which extracts lithium, forming a concentrated solution of lithium bicarbonate (Figure 14, Step 2). Since the concentration of the resulting lithium bicarbonate solution is higher than that of Li₂CO₃, by releasing the CO₂ pressure and heating to about 80°C, we have shown that the bicarbonate is quickly converted to carbonate leading to the Li₂CO₃ precipitate.

Complete regeneration of the sorbent can be achieved by continuously recirculating a small volume of carbonic acid solution between the sorbent column and a crystallizer. The difference in CO₂ pressure results in a pH swing that provides a driving force to pump the lithium out of the sorbent and deposit Li₂CO₃ powder in the crystallizer. We expect we will be able to produce high-purity Li₂CO₃ because impurities carried over from the adsorption step (e.g., sodium or potassium) will remain in solution as the Li₂CO₃ is selectively crystallized.

After regeneration with CO₂, the sorbent is conditioned with a solution of 0.1 M NaOH to convert the imprinted polymer into its Na⁺ form. For clarity, this step is not shown in Figure 14, but was taken in account in the process economics analysis.

The following parameters and assumptions were used in our process economics evaluation.

| | |
|-----------------------------------|-------------------------------|
| ▪ Brine flow rate: | 6000 gal/min |
| ▪ Recovery efficiency: | 90% |
| ▪ Lithium concentration in brine: | 400 ppm |
| ▪ Sorbent capacity: | 2g Li ⁺ /L sorbent |
| ▪ Sorbent cost: | \$33/Kg |
| ▪ Lithium production rate: | \$49 Kg/min |

Our estimates indicate that a minimum sorbent capacity of 2g Li⁺/L sorbent is needed in the separation process to effectively increase the lithium concentration in the sorbent. At our current polymer packing density of about 0.3 g/cc, 2g Li⁺/L sorbent is more than double than our current best capacity. However, we estimate that a capacity of at least 2g Li⁺/ L sorbent is achievable using a nanocomposite sorbent consisting of a nanostructured Li inorganic sieve, such as hydrous manganese oxide (HMO) or aluminum hydroxide, and the Li-imprinted polymer in the form of porous macrobeads. Specifically, to estimate the cost of the sorbent, we have assumed that the composite polymer sorbent beads will contain 50 wt% of HMO and 50 wt% of Li-imprinted polymer.

Furthermore, we have also assumed in our process design that the kinetics of the composite sorbent are similar to what we measured for the Li-imprinted polymer.

The estimated bulk sorbent cost is based on a cost of \$20/Kg of HMO¹ and \$46/Kg for the imprinted polymer. The cost of the imprinted polymer is based on a cost of \$20/Kg for a typical ion exchange resin plus an expected added cost of \$16/Kg from the preparation of the lithium chelating monomer². We also assume that the processing costs for the synthesis of a typical ion-

¹ Based on the cost of lithium manganese oxide spinel for lithium batteries.

² Assuming that 20% wt lithium chelating monomer is present in the polymer.

exchange resin and the composite sorbent are the same, and therefore already included in the cost of the ion-exchange resin.

Table A-1 in the Appendix summarizes the estimated cost for the equipment and fixed capital costs needed for the lithium extraction and Li₂CO₃ production. Costs were estimated according to the following:

- Sizing the columns based on known flow rates and assumed residence time.
- Simulating process design with Aspen software (Aspen Technology, Inc.).
- Estimating 2010 equipment costs from Towler & Sinnott “Chemical Engineering Design: principle, Practices and Economics of Plant and Process Design” and Peters, Timmerhaus & West, “Plant Design and Economics for Chemical Engineers.”
- Adjusting the equipment costs to 2015 values using the Chemical Engineering Plant Cost Index (CEPCI).
- Estimating the process building cost for the membrane system from “*Desalting Handbook for Planners* , 3rd edition, prepared by RosTek Associates, DSS Consulting, Inc. and Aqua Resources International, Inc., Desalination Research and Development Program Report No. 72 (United States Department of Interior, Bureau of Reclamation).

According to our estimates, the total plant cost is \$20,456,265.

Based on the operating items included in Table A-2 in the Appendix, the total annual operating cost is \$11,057,048 assuming 300 days/year uptime.

At a conservative sale price of \$2000/ton for Li₂CO₃, the annual revenue from the sale of Li₂CO₃ would exceed \$40,000,000 at a production rate of 49Kg/min.

CONCLUSIONS AND RECOMMENDATIONS

We have prepared and characterized several lithium- and manganese-imprinted polymers in the form of macrobeads with sizes of more than 200 micron. The polymers were tested both in batch extractions and in packed bed lab-scale columns at temperatures of 45-100°C. Lithium-imprinted polymers were found to have a Li adsorption capacity as high as 2.8 mg Li⁺/g polymer at 45°C, and manganese imprinted polymers were found to have a Mn adsorption capacity of more than 23 mg Mn²⁺/g polymer at 75°C.

The Li-imprinted polymers were found to have good extraction selectivity for Li⁺ in brines containing competing metal ions, such as Na⁺ and K⁺. The Li extraction efficiency of the Li-imprinted polymer was found to be more than 95% when a brine containing 390 ppm Li⁺, 410 ppm Na⁺, and 390 ppm K⁺ was passed through a packed bed of the polymer in a lab-scale column at 45°C. The polymer sorbent extraction efficiencies in brines with higher concentrations of Na⁺ and K⁺ were lower.

Further work needs to be done to increase both the capacity and selectivity of our current generation of Li-imprinted polymers by functionalizing the polymer with ligands with higher binding affinity for Li⁺ and by varying the content of crosslinking agent. Furthermore, we expect to develop better sorbents by producing a nanocomposite sorbent consisting of a nanostructured Li⁺ inorganic sieve and a Li-imprinted polymer. Our preliminary process cost analysis for the separation of Li and production of Li₂CO₃ supports the economics of our proposed process.

Manganese-imprinted polymers were also found to have good selectivity. The Mn extraction efficiency of the Mn-imprinted polymer from a synthetic brine containing several competing cations such as Li⁺, Na⁺, K⁺, Ca²⁺, Mg²⁺, and Ba²⁺ was found to be 72% at 75°C in a lab-scale column.

Further work on combining two different manganese binding ligands in the crosslinked polymer matrix is desirable to increase both the sorbent capacity and selectivity.

REFERENCES

1. Argonne National Laboratory Report ANL/EVS/R-10/5 “Water Use in the Development and Operation of Geothermal Power Plants”, by C.E. Clark et al., Jan 2011.
2. X. Shi et al., Hydrometallurgy 110 (2011) 99–106 and references therein
3. C. Branger et al., Reactive and Functional Polymers 73 (2013) 859-879.
4. “Lithium Process Chemistry”, 1st Edition, 2015, Ed. Chagnes and Swiatowska, Chapter 3.
5. “Handbook of Separation Process technology”, 1987, Ed. Ronald W. Rousseau, Chapter 13.

APPENDIX

Table A1
ESTIMATED COST FOR EQUIPMENT AND FIXED CAPITAL COSTS

| Equipment | Value | Unit | Equipment costs, Jan 2010, from Towler & Sinnott | Adjusted for plastic-lined steel instead of carbon steel (factor of 2) | Equipment costs, adjusted to 2016 value using CEPCI index |
|--|-------------|--------|--|--|---|
| Absorber (Column 1) | | | | | |
| <u>Column</u> | | | | | |
| Diameter | 12 | m | | | |
| column height | 3 | m | \$180,886 | \$361,772 | \$509,188 |
| <u>Pump brine to column</u> | | | | | \$0 |
| head | 100 | ft | | | \$0 |
| pump flow rate (upper absorber recirculation pump) | 378.3333333 | L/s | \$58,153 | \$116,306 | \$121,523 |
| Regenerator (Column 2) | | | | | \$0 |
| <u>Column</u> | | | | | \$0 |
| regenerator column diameter | 12 | m | | | \$0 |
| column height | 3 | m | \$180,886 | \$361,772 | \$509,188 |
| <u>Crystallizer (Steam Heated)</u> | | | | | \$0 |
| Volume | 25 | m3 | \$149,700 | \$299,400 | \$289,370 |
| <u>Lean/Rich Heat Exchanger</u> | | | | | \$0 |
| Exchanger duty | 6.52E+07 | Btu/hr | | | \$0 |
| Exchanger area | 1113 | m2 | \$127,834 | \$255,669 | \$267,135 |
| | | | | | \$0 |
| <u>Compress CO2 to Column 2</u> | | | | | \$0 |
| compressor duty (kW) | 174 | kW | \$114,053 | \$114,053 | \$160,528 |
| <u>Pump water from reboiler to Column 2</u> | | | | | \$0 |
| pump flow rate | 81.66666667 | L/s | \$20,620 | \$41,240 | \$43,089 |
| <u>Cooler for CO2/water entering Column</u> | | | | | \$0 |

| <u>2</u> | | | | | | |
|--|-------------|-----------------|-----------|--------------|--|-------------|
| Cooling duty - lean stream cooler | 2.46E+07 | Btu/hr | | | | \$0 |
| Exchanger area | 762 | m ² | \$89,566 | \$179,131.68 | | \$187,166 |
| Solids Handling | | | | | | \$0 |
| <i><u>Centrifugal Separator</u></i> | | | | | | |
| Solids rate | 49 | kg/min | \$369,600 | \$369,600.00 | | \$386,176 |
| <i><u>Crusher/Grinder</u></i> | | | | | | \$0 |
| Solids rate | 2.94 | ton/h | \$349,524 | \$349,524.03 | | \$365,200 |
| <i><u>Dryer</u></i> | | | | | | \$0 |
| Solids rate | 2.94 | ton/h | \$283,500 | \$283,500.00 | | \$296,215 |
| <i><u>Packaging</u></i> | | | | | | \$0 |
| Solids rate | 2.94 | ton/h | \$2,030 | \$2,030.00 | | \$4,327 |
| NaOH equipment | | | | | | |
| <i><u>Pump NaOH solution into column</u></i> | | | | | | \$0 |
| pump flow rate | 383.3333333 | L/s | \$58,749 | \$117,499 | | \$122,768 |
| <i><u>NaOH Storage Tank</u></i> | | | | | | \$0 |
| Tank volume | 2193 | m ³ | \$146,811 | \$293,622 | | \$413,268 |
| Pre-Filtration | | | | | | \$0 |
| <i><u>Solids removal filter (x2)</u></i> | | | | | | \$0 |
| Filter area | 160 | ft ² | \$177,400 | \$177,400 | | \$185,356 |
| Sum of Equipment Costs | - | | | | | \$3,860,496 |

Table A2
ESTIMATED OPERATION EXPENSES

| Operating Input | | | | Operating Costs (\$/hour) |
|--|--------------|--|--------------|----------------------------------|
| Sorbent | 70 | tonne | | |
| | 233.33333333 | m3 based on 0.3 g/cc packing density | | |
| | 233333.3333 | L per year assuming 1 year replacement | | |
| | 26.63622527 | L/h | \$10.0000000 | \$266.36 |
| | | | | |
| CO₂ makeup | 2400 | kg/h | \$0.0500000 | \$120.00 |
| | | | | |
| NaOH for resin conditioning | 107.0592 | kg/h | \$0.4000000 | \$42.82 |
| | | | | |
| Acid for neutralizing spent NaOH | 136.7514 | kg/h | \$0.2500000 | \$34.19 |
| | | | | |
| Makeup water for resin conditioning | 85720 | kg/h | \$0.0004413 | \$37.83 |
| | | | | |
| Waste treatment | 85720 | kg/h | \$0.0015000 | \$134.35 |
| | | | | |
| Cooling water (cooler on Column 2 feed) | | | | |
| | 1243549.39 | kg/h | \$0.0000044 | \$5.48 |
| | -24632639.78 | Btu/h | | |
| | 5.51 | \$/h | | |
| | | | | |
| Heat exchanger | | | | |
| | 64354601.56 | Btu/hr | | |
| | | | | |
| Steam (assume that required heat input to the crystallizer equals | | | | |

| | | | | |
|--|-------------|------------------------------------|-------------|-----------------|
| twice the required cooling water input to the Column 2 feed) (The heat input from CO₂ compression is very small comparatively) | | | | |
| latent heat of steam at 125C (19 psig) | 2188 | kJ/kg | | |
| latent heat of steam at 125C (19 psig) | 941 | Btu/lb | | |
| Steam needed at 125 C (19 psig) | 52354.17594 | lb/h | | |
| latent heat of steam at 150 psig (185 C) | 1994 | kJ/kg | | |
| latent heat of steam at 150 psig (185 C) | 858 | Btu/lb | | |
| steam needed at 150 psig (185 C) | 57418.74075 | lb/h | \$0.0019976 | \$162.05 |
| Electricity | | | | |
| P-1 | 121 | kW | \$0.0700000 | \$8.47 |
| P-2 | 113 | kW | \$0.0700000 | \$7.91 |
| Centrifugal separator | 100 | kW | \$0.0700000 | \$7.00 |
| Compressor | 282 | kW | \$0.0700000 | \$19.74 |
| Crusher/Grinder | 22 | kW | \$0.0700000 | \$1.54 |
| Dryer | 50 | kW | \$0.0700000 | \$3.50 |
| Packaging | 0.75 | kW | \$0.0700000 | \$0.05 |
| Maintenance | | | | |
| Annual cost for equipment maintenance/repair | 7 | % of fixed capital investment/year | | \$13.57 |
| Operating Labor (estimated from Peters, Timmerhaus, & West textbook) | | | | |
| employee hours/hour | 3 | hours/h | \$28.52 | \$85.56 |
| Supervisory/Clerical Labor | | | | |
| Ratio factor | 0.15 | \$/\$/ operating labor | | \$12.83 |
| Operating supplies | | | | |
| Ratio factor | 0.15 | \$/\$/ maintenance | | \$2.04 |
| Laboratory charges | | | | |
| Ratio factor | 0.1 | \$/\$/ operating labor | | \$8.56 |
| Fixed charges | | | | |
| Ratio factor | 0.1 | \$/\$/ total product cost | | \$51.05 |

| | | | | |
|---|------|---------------------------|----------------------|---------------------|
| Administrative Costs | | | | |
| Ratio factor | 0.15 | \$/\$/ operating labor | \$12.83 | |
| Distribution/Marketing Costs | | | | |
| Ratio factor | 0.02 | \$/\$/ total product cost | \$11.49 | |
| Research & Development Costs | | | | |
| Ratio factor | 0.05 | \$/\$/ total product cost | \$28.72 | |
| Nanofiltration operating costs | 6000 | gal/min | Year 2000 cost basis | |
| | 360 | 1000 gal/h | \$0.90 | \$457.76 |
| | | | | |
| | | | | \$1,536 |
| | | | | \$11,057,048 |